

Orion: A Fully Homomorphic Encryption Compiler for Private Deep Neural Network Inference

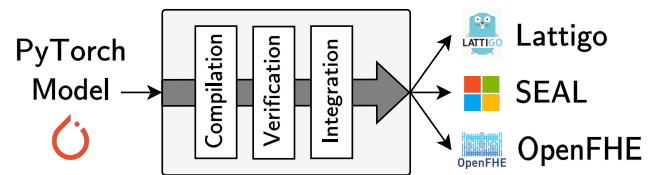
Austin Ebel*, Karthik Garimella*, Brandon Reagen
New York University
{abe5240,kg2383,bjr5}@nyu.edu

Abstract—Fully Homomorphic Encryption (FHE) has the potential to substantially improve privacy and security by enabling computation on encrypted data. This is especially true with deep learning, as today many popular user services are powered by neural networks. One of the major challenges facing wide-scale deployment of FHE-secured neural inference is effectively mapping them to the FHE domain. FHE poses many programming challenges including packing large vectors, handling expensive rotations, and correctly implementing complex strided convolutions. This makes programming FHE inferences prone to poor performance and errors. In this paper we overcome these challenges with Orion, an automated optimizing FHE compiler for neural inference. Orion automatically maps PyTorch-specified networks to FHE, handling common layer types and arbitrary tensor shapes and strides. Moreover, we develop novel optimizations that balance dense FHE vector packing, efficient rotations, and minimize operations to improve performance. We have implemented Orion, which will be open sourced, and evaluated it on common benchmarks used by the FHE deep learning community. We compare Orion to multiple state-of-the-art solutions and report iso-accuracy speedups ranging from $2.7\times$ to $20.5\times$.

I. INTRODUCTION

The steady increase of outsourced cloud computing services has given rise to concerns surrounding data privacy, which dictate how and when personal data is collected, viewed, and used. Furthermore, privacy and security risks are intensified by data-hungry cloud-based machine learning services that operate on large volumes of user data. Traditional cryptographic methods protect data during transmission and storage but must be decrypted in the cloud for processing, thus exposing data to wrongful use or access. Privacy preserving computation (PPC) overcomes this by safeguarding user data *during* computation, ensuring that data remains encrypted throughout the process. Fully Homomorphic Encryption (FHE) is a prominent PPC solution that provides secure cloud computation, enabling functions to be computed on encrypted data without first decrypting. In this manner, the client’s data, and any outputs obtained processing their data, remain encrypted and can only be observed in the clear when the client locally decrypts it using their secret key.

FHE has broad applications ranging from finance to health and other situations involving sensitive data. Many of these services are now driven by deep learning, specifically neural networks. Thus, prior work, and our work here, has focused on optimization techniques to facilitate more efficient



Listing 1 PyTorch integration with Orion.

```
1 net = ResNet20()
2 net.eval()
3 pred_clear = net(img) # Forward pass (PyTorch).
4
5 net.compile() # Generate HE representation.
6 net.he() # Set to HE mode.
7 pred_he = net(img) # HE-friendly inference.
```

processing of deep learning with FHE. Despite this, the wide-scale deployment of FHE-enabled private deep learning is limited by extremely high computational costs and programming challenges of translating plaintext programs to the constraints of FHE. This has given rise to two major thrusts of research: hardware accelerators to provide the raw computational performance needs [1]–[6] and compilers to effectively translate programs [7]–[11], which is also essential for high performance. This paper focuses on automatically and efficiently mapping neural networks to FHE.

Multiple compounding factors make effectively mapping neural networks to FHE challenging. First, operands in FHE are very large vectors. These vectors range from lengths of 1024 to 128K, with recent work favoring the larger lengths [3], [5]. Scalar data are packed into these vectors but cannot be individually indexed nor partial vectors processed; any function applied to a vector is applied to all elements. Therefore, each function (i.e., addition and multiplication) is computationally expensive and if vector elements (i.e., *slots*) are not utilized, performance degrades. This makes it imperative to optimize data packing and layout into FHE vectors. Next, vector elements can be realigned via rotations. However, these rotations are highly computationally expensive as each entails a *key-switch* operation, which can dominate runtime [3], [12]. Finally, each encrypted vector can only execute finite computations before decryption fails. To prevent this, bootstrapping can be used to reset computation support but comes at an extremely high latency cost [13]. Therefore,

*Equal contribution.

careful attention must be placed on the amount and type of operations performed on FHE vectors. Not only are each of the above problems difficult to address individually, but they also have competing objectives. For example, the most dense packing strategies have the highest slot utilization but necessitate frequent bootstrapping operations. This makes for a complex optimization landscape and motivates the need for a robust and automated infrastructure.

To address these challenges we present Orion, an automated and optimizing compiler for translating plaintext neural networks to FHE. As a compiler, Orion takes as input neural network descriptions written in PyTorch [14] and generates FHE programs written in Lattigo [15]. This process is shown in Listing 1. Orion supports major neural network layers (e.g., fully-connected and convolution) and, for the first time, handles strided convolutions automatically. Orion also includes a set of novel optimizations to speedup neural inference under FHE. First, we develop three distinct vector packing strategies tailored to needs of individual neural network layers. Each strategy is tailored for the unique tradeoff in slot utilization and computational complexity. Second, we consider recent hoisting [13] optimizations to significantly speedup rotations. The insight is that rotating the same vector is far faster than rotating distinct ones; Orion leverages this by optimizing how data is packed and rotations are scheduled. Third, we develop a technique to reduce the number of levels needed to perform a computation by introducing structured sparsity into ciphertexts. By saving levels, we can significantly reduce the number of bootstrapping calls. Finally, we observe that there is a tradeoff between hoisted input rotations and non-hoisted output rotations wherein a few output rotations can save hundreds of hoisted ones. We explore and optimize this tradeoff natively in Orion.

We evaluate Orion using a set of neural networks and microbenchmarks to highlight the intuitions behind the optimizations and approaches. In many cases, we find that the densest packing strategies are not always the most efficient. We compare Orion to two distinct state of the art approaches and report significant speedup. Orion, and all benchmarking infrastructure, will be open-sourced.

We make the following contributions:

1. We develop Orion: an automated optimizing compiler for FHE neural network inference that directly integrates into PyTorch.
2. A collection of new FHE linear algebra techniques that handle arbitrary matrix-vector products and data layout.
3. A suite of FHE linear layer microbenchmarks that target both commonly deployed convolutional and linear layers as well as a set of more challenging and non-standard layers. Benchmarking Orion, we outperform the state-of-the-art FFT-based and rotation-based algorithms by $2.7\times$ and $20.5\times$ at iso-accuracy, respectively.

II. A PRIMER ON FHE AND DEEP LEARNING

In this section we provide a review of the core concepts of FHE and deep learning needed to understand the contributions

TABLE I: CKKS Parameters.

| Param. | Description |
|------------------------------------|--|
| \mathbf{m} | Message, a vector of real or complex numbers. |
| $[\mathbf{m}]$ | Plaintext polynomial encoding the message, \mathbf{m} . |
| $\llbracket \mathbf{m} \rrbracket$ | Ciphertext encrypting the plaintext polynomial, $[\mathbf{m}]$. |
| N | Power-of-two polynomial ring degree. |
| n | Length of the vector message, $n \leq N$ (or $N/2$). |
| L | Maximum multiplicative level of $\llbracket \mathbf{m} \rrbracket$. |
| ℓ | Current multiplicative level. |
| Q | Initial polynomial modulus. |
| q_i | Small moduli in RNS decomposition of $Q = \prod_{i=0}^L q_i$. |
| P | Auxiliary modulus used in key-switching. |
| Δ | Scaling factor applied to $\llbracket \mathbf{m} \rrbracket$. |
| L_{boot} | Number of levels consumed by bootstrapping. |
| L_{eff} | Maximum achievable level after bootstrapping. |

and insights of Orion. We begin by reviewing FHE and specifically the CKKS [16] scheme, which is widely used for deep learning. Next, we briefly review deep neural networks.

A. Fully Homomorphic Encryption

Since the first FHE scheme was developed in 2009 [17] many algorithmic optimizations have been proposed to steadily improve performance. A variety of schemes now exist including BGV [18], BFV [19], [20], and CKKS [16]. At a high-level many of the characteristics are the same. For example, they are all based on the Ring Learning with Errors (RLWE) problem [21], support addition, multiplication, and rotations and work over large vectors. Recently, CKKS has emerged as the dominant scheme for deep learning in part due to its native support of fixed-point arithmetic. We target CKKS with Orion and detail it here.

1) *CKKS Notation:* We list the relevant CKKS parameters in Table I. To perform FHE operations, a vector message, \mathbf{m} , is converted into a fixed-point (integer) representation in part by multiplying the message with a large scaling factor, Δ . This encoded plaintext message, which we denote as $[\mathbf{m}]$, is an element of the polynomial ring $R_Q = \mathbb{Z}_Q[X]/(X^N + 1)$. In essence, this is another vector of length N , where each element is modulo some large value, Q . As we will see, the choice of N is largely application-dependent and is tied directly to the security of the scheme. For a polynomial with N coefficients, the corresponding vector must be of length $n \leq N$ for the specific class of problems we explore in future sections, and $n \leq N/2$ otherwise. Following prior work, we refer to n as the number of *slots* that the polynomial can encode. A core challenge in designing efficient HE algorithms is finding a way to tightly pack data within vector messages to take full advantage of the SIMD-like parallelism provided by the slots. Poor mapping strategies can result in ciphertexts with unused slots, which we refer to as slot underutilization throughout.

2) *Ciphertext Structure:* Depending on a problem’s complexity, the value of Q can range from hundreds to thousands of bits. For efficiency, polynomials are decomposed into an equivalent RNS (*residue number system*) representation consisting of many smaller, machine-word size moduli, q_i , such

that $q_0 \times q_1 \times \dots \times q_L = Q$. Here, L is the maximum multiplicative level of the polynomial, and several homomorphic operations consume levels to ensure the scales of polynomials remain in check. Therefore, at any given time, a polynomial can be at level ℓ , such that $0 \leq \ell \leq L$, and we refer to ℓ as the remaining number of levels in the polynomial.

A ciphertext, $[[\mathbf{m}]]$, consists of a pair of polynomials $([\mathbf{a}], [\mathbf{b}])$, where the underlying vector message is encoded in one of the polynomials alongside the addition of a small amount of random noise to ensure the security of the RLWE scheme. We sometimes refer to a ciphertext as $[[\mathbf{m}]]_s$ to explicitly indicate that $[[\mathbf{m}]]$ is encrypted under secret key, s . As with any FHE scheme, operations performed on ciphertexts have an equivalent effect on the underlying vector message.

3) *FHE Operations*: We now briefly describe the available operations that can be performed in the CKKS domain.

Addition CKKS supports point-wise addition between one plaintext and one ciphertext or between two ciphertexts. When performing addition, each operand must be at the same number of levels, ℓ . Following convention from [3], we refer to plaintext-ciphertext addition as PAdd and ciphertext-ciphertext addition as HAdd. Both PAdd and HAdd output a ciphertext.

Algorithm 1 $\text{PMult}([[x]], [y]) = [z]$

- 1: $[\mathbf{a}], [\mathbf{b}] := [[\mathbf{x}]]$ ▷ Scale: Δ , Level: ℓ
 - 2: $[z] := [\mathbf{a} \cdot \mathbf{y}], [\mathbf{b} \cdot \mathbf{y}]$ ▷ Scale: Δ^2 , Level: ℓ
 - 3: $[z] := \text{Rescale}([z])$ ▷ Scale: Δ , Level: $\ell - 1$
 - 4: **return** $[z]$
-

Multiplication Similar to addition, CKKS also supports point-wise multiplication between one plaintext and one ciphertext or between two ciphertexts. These operations are referred to as PMult and HMult, respectively. Since model weights need not be encrypted server-side, many of the computations in private neural network inference are PMults where the plaintext represents the weights of a particular layer and the ciphertext represents the client’s input to that layer. Finally, recall that messages are encoded with an associated scaling factor, Δ . Therefore when two polynomials are multiplied, the resulting scale increases to Δ^2 , as is typical in fixed-point arithmetic. CKKS supports a Rescale procedure that reduces this scale back to roughly Δ at the cost of consuming one level in the resulting ciphertext. This rescaling operation is shown for PMult in Algorithm 1.

Algorithm 2 $\text{HRot}([[x]], r, \text{swk}_r) = [y]$

- 1: $[y]_{s'} := \psi_r([[x]]_s)$ ▷ Secret key: s'
 - 2: $[y]_s := \text{KeySwitch}([y]_{s'}, \text{swk}_r)$ ▷ Secret key: s
 - 3: **return** $[y]$
-

Rotation CKKS also supports ciphertext rotations, denoted as HRot, in which a permutation to the polynomial coefficients, ψ_r is performed for a given rotation amount, r . This has the effect of cyclically shifting elements in the underlying vector message by r positions. Rotations transform

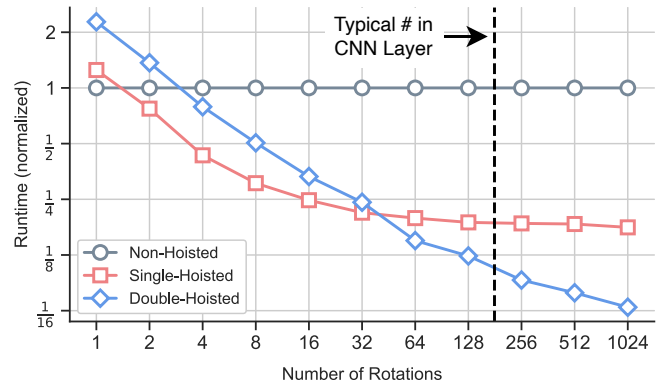


Fig. 1: Performance comparison of single and double-hoisted rotations relative to non-hoisted rotations.

the ciphertext in such a way that it cannot be decrypted by the original secret key, s . Therefore an expensive *key-switching* step is required to convert the ciphertext back to being decryptable by s . This involves performing numerous number theoretic transforms (NTTs, the finite field equivalent of FFTs), and RNS basis extensions before multiplying with a large switching key, swk . HRot is shown in Algorithm 2.

Hoisting: Recently, a performance optimization was developed to amortize rotations to the same ciphertext. When the *same* ciphertext is rotated by different amounts, one can *hoist* out these expensive operations and perform them significantly fewer times. The act of (single) hoisting was originally proposed by Halevi and Shoup [22] and further optimized by Bossuat et al. [13] in a double-hoisting procedure. Figure 1 illustrates the performance difference between non-hoisted, single-hoisted, and double-hoisted rotations as the number of rotations on the same ciphertext is varied. We find double-hoisting to be 10× (2×) faster than non-hoisted (single-hoisted) rotations that are present in typical CNN layers. Unlike prior work, Orion optimizes mapping strategies to take full advantage of the performance benefits offered by hoisting, sometimes at the cost of slot underutilization.

Bootstrapping Finally, for a scheme to be *fully* homomorphic, it must include a way of *increasing* the number of remaining levels; the Bootstrap operation provides this functionality. Bootstrapping is a computationally demanding procedure that increases levels but also consumes a fixed number (L_{boot}) of levels in the process. A ciphertext that began at level L can only reach an effective level, $L_{\text{eff}} = L - L_{\text{boot}}$ after bootstrapping. A typical L_{boot} is 15 levels [13].

B. Deep Learning

Orion targets convolutional neural networks (CNNs), a class of feed-forward neural networks that consist of a series of linear and non-linear transformations applied to an input image. Below, we set up our notation and describe each type of computation we support.

1) *Linear Layers*: Each linear transformation is either a convolution, fully-connected matrix-vector product, or an average pooling operation. We develop FHE linear algebra kernels for performing matrix-vector products, and as we will

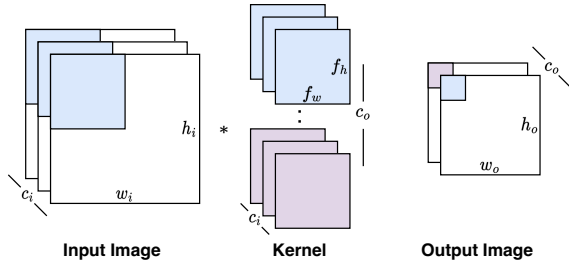


Fig. 2: Orion supports the multiple-input multiple output channel (MIMO) convolution that is present in standard CNN networks such as ResNets.

show, express convolutions as a matrix-vector product, thus supporting all aforementioned linear operations in Orion.

Convolution A convolutional layer consists of an input image of size $h_i \times w_i \times c_i$ that is processed through a set of trainable filters of size $f_h \times f_w \times c_i$. These filters perform element-wise weighted-summations over localized regions between the image pixels and the kernel values to produce a single output pixel. The convolution layer is also defined by a stride (s_h, s_w) , which denotes the number of pixels the kernel shifts over in each spatial dimension when performing the weighted-sum. The convolution is further parameterized by a padding parameter (denoted as p) that adds a set of p zeros to each side of the input image to increase the resolution of the output image. In order to produce multiple output channels, there will be c_o sets of the filters that are independently applied to the input image to produce an output image of size $h_o \times w_o \times c_o$. Finally, there is a separate bias term for each of the c_o output channels. Orion supports the multiple-input multiple-output channel case shown in Figure 2.

Average Pooling Average Pooling Layers are a special case of convolutions with a kernel size of $f_h \times f_w$ where every filter value is $1/(f_h \cdot f_w)$. Usually, $s_h, s_w > 1$ in order to decrease the image resolution by a factor of $s_h \times s_w$.

Fully-Connected Layers An input vector of size n_i is transformed via a trainable weight matrix of size $n_o \times n_i$ to produce an output vector of size n_o . Additionally, we add a bias term of size n_o to the output of the matrix-vector product.

2) *Non-linear Layers*: CKKS only supports addition and multiplication and therefore cannot support common non-linear activation functions such as ReLU. To this end, Orion supports the use of polynomial activation functions [23]–[25].

III. THE ORION COMPILER

In this section, we provide an overview of the Orion compiler, review common FHE matrix-vector products, and introduce our proposed optimizations.

A. Orion

Orion is composed of three distinct phases: compilation, verification, and integration. First, a user specifies their network architecture in PyTorch, which is then directly compiled

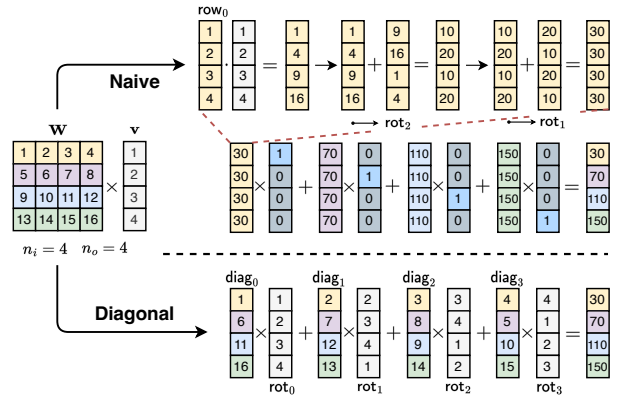


Fig. 3: The Naive and Halevi-Shoup Diagonal methods for performing matrix-vector products under FHE. Halevi-Shoup diagonalization techniques removes the need for expensive output rotations.

and transformed into a set of layer-wise FHE-equivalent operations as shown in Listing 1. Orion takes three passes over the network specification. The first pass collects input and output tensor dimensions for each layer as well as layer type. The second pass generates the necessary FHE representation to perform FHE transformations. The final pass prunes any unnecessary level consumption by examining network inference under the aforementioned intermediate representation. From here, the user can verify correctness of the underlying FHE forward-pass implementation by simulating the FHE inference directly in PyTorch, thus easing the development process. Finally, the generated representation is interpreted by an FHE library (we currently support Lattigo) to run FHE inference in the CKKS scheme.

Similar to prior work, we assume a semi-honest threat model between the two parties meaning that the parties may be corrupted by an adversary, but the adversary is passive and will follow the prescribed protocol. Furthermore, this adversary will try to learn as much private information as they can from the data they receive throughout the faithful execution of the protocol. Finally, Orion always operates at 128 bit security by choosing the appropriate FHE parameters.

B. FHE Matrix Operations

We now present mapping strategies for computing FHE matrix-vector with CKKS. We review prior strategies and then show our three methods: Square, Hybrid++, and Partitioned. We divide each strategy into three stages: Setup, Core, and Repair. Since Orion handles both fully-connected and convolutional layers, we also explain our conversion strategy for efficiently expressing convolutions as matrix-vector products. We note that linear transformations performed in Lattigo further reduce the number of rotations by performing a baby-step giant-step algorithm (see Algorithm 6 of [13]). Unless stated otherwise, we assume input and output sizes are powers of two and that all input and output data fits in a single ciphertext.

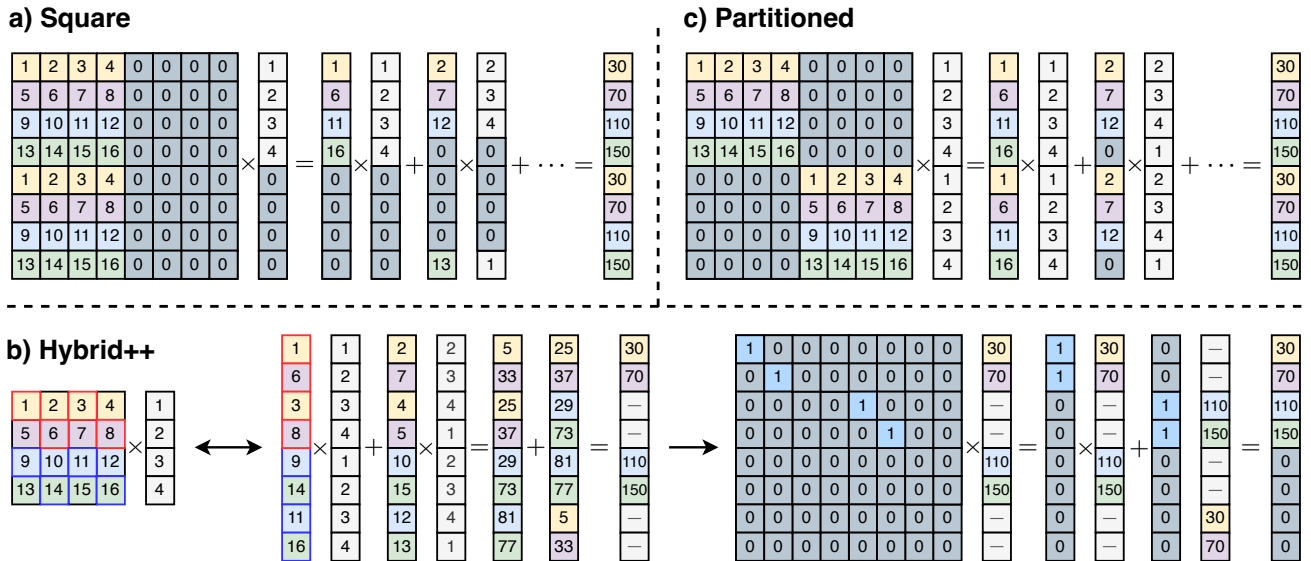


Fig. 4: An overview of our three proposed mapping strategies. Note that the Hybrid++ method tightly packs vectors at the cost of performing two sequential matrix-vector products thus consuming an additional level.

Naive HE Matrix-Vector product. We begin with the most straightforward but also most inefficient method for performing FHE matrix-vector products.

Setup: Each row of the weight matrix \mathbf{W} is encoded as a separate plaintext polynomial.

Core: Each of these n_o polynomials is first multiplied by $[\mathbf{v}]$ using PMult (the first row’s PMult is shown in Figure 3). The resulting output ciphertext then contains each of the partial sums for its corresponding dot product. In order to obtain the full dot product, each ciphertext then goes through a series of rotation-and-summations. This process is shown at the top of Figure 3 for the first row, in which two rotations-and-summations are required to align all elements of the ciphertext to produce the dot product. Notably, these output rotations cannot be hoisted out as they are applied to intermediate outputs of the rotation-and-summations.

Repair: Each of the n_o final ciphertexts must be combined into a single ciphertext. This process itself requires n_o many PMult calls between resulting ciphertexts and a selector polynomial (a one-hot vector set appropriately) and finally $n_o - 1$ HAdd calls to produce the desired ciphertext. This process is shown in the middle row of Figure 3.

The Halevi-Shoup Diagonal Approach. At a high level, this algorithm processes the matrix in a diagonal order so that each slot in an intermediate ciphertext contains a partial sum from a different row of the weight matrix. Therefore, Halevi-Shoup avoids the need to perform the expensive output rotations that were necessary in the Naive method.

Setup: Since the server has access to the plaintext weight matrix \mathbf{W} , the server is able to first reconfigure the weight matrix without incurring any HE overhead. In particular, the server can first extract the generalized diagonals of their weight matrix in the plaintext domain. The diagonals are expressed as $\text{diag}_k = W_{[0,k]}, W_{[1,1+k]}, \dots, W_{[n_i-1, n_i-1+k]}$ where the

second dimension index is computed modulo n_i , and each of the n_o many diagonals will be of length n_i . The generalized diagonals are then encoded as separate plaintext vectors. The four extracted diagonals for the example matrix are shown in bottom row of Figure 3.

Core: We can now perform PMult between the encoded diagonals and the input ciphertext $[\mathbf{v}]$. Since diag_k begins with a weight element in column k of \mathbf{W} , the input ciphertext is rotated up by k slots in order to align the plaintext diagonal and the ciphertext. For example, diag_2 is multiplied by the input ciphertext rotated up by 2 slots. These rotations can be hoisted out since they are applied to the input ciphertext. This process will produce n_o intermediate ciphertexts that contain the partial sums of the matrix-vector product. Finally, the ciphertexts can simply be added together using HAdd to produce a single ciphertext corresponding to the desired matrix-vector product as shown in Figure 3 (bottom row).

Repair: In the example shown above, the Halevi-Shoup algorithm does not require post-processing as the resulting ciphertext is already tightly packed.

Proposed Method 1: Square. In the Naive and Halevi-Shoup algorithms, we have not taken into consideration the full ciphertext structure. In particular, recall from Section II-A that messages are necessarily encoded in a fixed number of slots, n , and often, n is typically much larger than the either dimensions of \mathbf{W} . Therefore, to produce a valid matrix-vector product in FHE, we must modify our matrix such that it always has n columns.

In the Square method, we embed a weight matrix \mathbf{W} of size $n_o \times n_i$ inside a larger matrix of size $n \times n$ (slots-by-slots). Here, n_i need not be equal to n_o . We visualize this in Figure 4a, where $n_i = 4, n_o = 8$, and $n = 8$. This direct embedding produces many relatively sparse diagonals, each which must be multiplied with the input vector rotated by

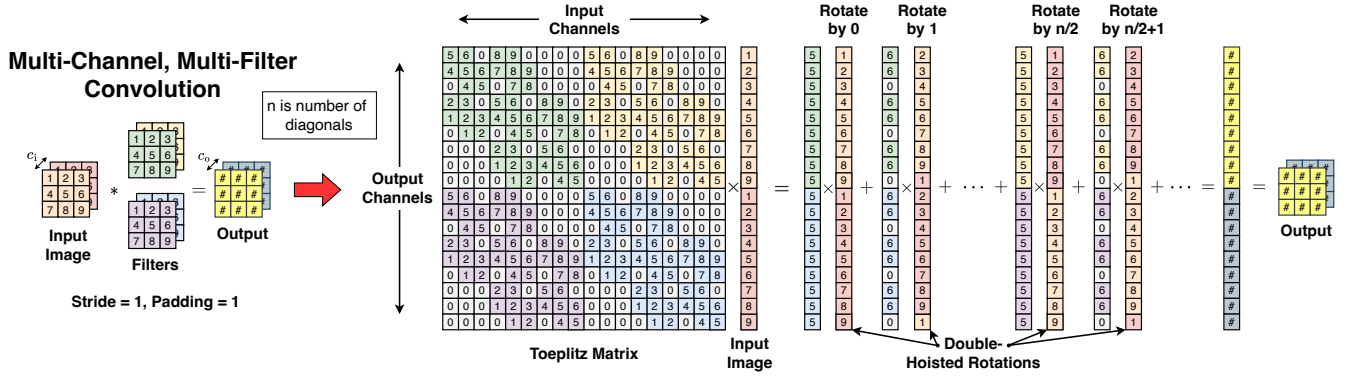


Fig. 5: Visualizing the $kn2col$ method for converting general convolutions to matrix-vector products.

the correct amount. However, each of these rotation can be double-hoisted and therefore their cost can be amortized.

Setup: We embed our $n_o \times n_i$ weight matrix \mathbf{W} into an $n \times n$ matrix given that $n_i, n_o < n$.

Core: We now extract the generalized non-zero diagonals. That is, any generalized diagonal that contains a non-zero element. We now proceed with the standard Halevi-Shoup algorithm to perform the matrix-vector product.

Repair: The first n_o many slots of the output ciphertext contains the desired matrix-vector product as shown in Figure 4a and does not need any post-processing.

Proposed Method 2: Hybrid++ Rather than producing many sparse diagonal as was the case in the Square method, we can attempt to pack diagonals more tightly in order to minimize the number of rotations. To this end, we extend Gazelle’s [26] input-packed Hybrid method to work in the FHE domain. In particular, Gazelle’s overall inference protocol allows for a resulting ciphertext from a matrix-vector product to be sent to the client who can decrypt, tightly pack, re-encrypt, and transmit a fresh ciphertext back to the server. In our FHE-only setup, there is no communication between the two parties until the forward pass is complete. Therefore in our setup, the server must 1) perform the tight repacking directly on the resulting ciphertext and 2) take into consideration the remaining levels in the ciphertext. If all levels are *consumed*, then the server must perform bootstrapping to proceed.

Setup: The weight matrix \mathbf{W} is of size $n_o \times n_i$, which is visualized in Figure 4b, with $n_o = 4, n_i = 4$, and $n = 8$. To fully utilize the n slots per polynomial, we split the weight matrix \mathbf{W} into s sub-matrices each of size $n_o/s \times n_i$. We then extract and concatenate the generalized diagonals of each sub-matrix such that the total length of a generalized diagonal is n . Figure 4b show the two extracted and concatenated generalized diagonals for our example matrix. Finally, we perform input duplication using rotation-and-summations in order to fill the ciphertext with copies of the input vector $[\mathbf{v}]$.

Core: Now, we can perform the Halevi-Shoup algorithm on these extracted diagonals by properly rotating the input ciphertext and calling PMult. However unlike Halevi-Shoup, we must perform $\log(s \cdot n_i/n_o)$ output rotations in order to align the partial sums for a particular row resulting in a

ciphertext that contains the desired outputs. As shown in Figure 4b, the outputs are not tightly packed in the first n_o slots of the resulting ciphertext.

Repair: To proceed in the following layer, the desired outputs must be re-aligned to the top n_o slots of the final ciphertext. We make use of a *permutation matrix* to 1) select and tightly pack the appropriate slots of the resulting ciphertext into the first n_o slots of the final ciphertext and 2) zero out the remaining $n - n_o$ slots. Importantly, this aligning and re-packing method consumes a level as this stage itself requires a matrix-vector product.

Proposed Method 3: Partitioned. The Partitioned method strikes a balance between the Square and Hybrid++ methods by more tightly packing the diagonals without consuming an additional level. This approach is visualized in Figure 4c, where $n_i = 4, n_o = 8$, and $n = 8$.

Setup: We first split the weight matrix \mathbf{W} into n_o/n_i many sub-matrices, each of size $n_i \times n_i$, which are then diagonally aligned inside of an $n_o \times n$ matrix. While this method produces generalized diagonals which are more sparse than the Hybrid++ approach, it preserves the row order of the weight matrix and therefore does not require an auxiliary permutation matrix. We again properly align the input ciphertext with each generalized diagonal.

Core: We perform PMult between the generalized diagonals and the input-rotated ciphertext. Finally, the resulting intermediate ciphertexts can be combined using HAdd, resulting in a tightly packed ciphertext containing the desired output.

Repair: If $n_o \neq n$, then it is necessary to perform output rotation-and-summations similar to the Hybrid++ method in order to combine the appropriate partial sums.

C. Expressing Convolutions as Matrix-Vector Products

In order to perform private CNN inference, we must first transform all convolutional layers into matrix-vector products that are amenable to FHE, and the de-facto approach is *im2col* (*image-to-column*). However, *im2col* requires heavy re-structuring of the input ciphertext and thus incurs a large overhead under FHE.

Therefore, an ideal algorithm for converting convolutions to matrix-vector products in an FHE setting is one that keeps

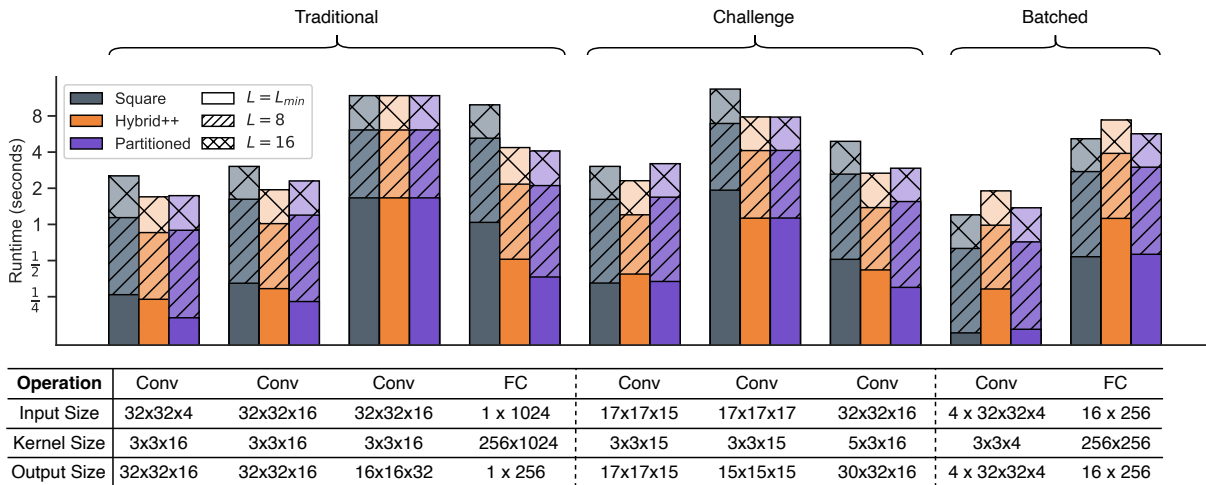


Fig. 6: Overview of Orion’s performance on our microbenchmarks for the three proposed mapping strategies.

the encrypted output of the previously layer as a vector in raster-scan fashion and *instead* expands the kernel to form the correct matrix. This less-common technique is known as *kn2col* (*kernel-to-column*), and we refer to the resulting matrices as *Toeplitz* matrices following the convention of [27]. To the best of our knowledge slytHERin [28] is the only prior work which proposes a similar strategy. We visualize the conversion from a traditional convolution to a matrix-vector product using the *kn2col* method in Fig 5, where $c_i = c_o = 2$, $w_i = h_i = 3$, $f_w = f_h = 3$, with padding and stride both set to 1. In general, the *kn2col* matrix will be of size $c_o w_o h_o \times c_i w_i h_i$, with each row corresponding to one filter multiplication.

There are several benefits of thinking about expressing convolutions as matrix-vector products using *kn2col*. First, this method produces *dense* diagonals, and since the number of hoisted ciphertext rotations is equal to the number of diagonals in a matrix-vector product, dense diagonals ensure a minimal number of rotations. Second, distinct filter elements lie along the same diagonal. In effect, this guarantees that the number of diagonals is *independent* of the size of the input or output image and instead only depends on filter size. We close with one implementation detail. Since strided convolutions create *punctures* in the underlying ciphertext, it is important to fill these punctures with computations from other independent convolutional filters. To this end, we adopt a “multiplexed” packing technique similar to Lee et al. [29] which consumes an additional level per convolution as we must undo this packing for future layers.

IV. EVALUATION

In this section, we begin by describing our experimental setup. Next, we run a set of microbenchmarks through Orion to better understand trade-offs between level consumption, mapping strategies, and hoisted versus non-hoisted rotations. Then, we evaluate Orion on different neural networks and compare performance against prior solutions, and finally we

explore the interplay between packing density and rotation procedure.

A. Evaluation Setup

We evaluate Orion using an r7g.16xlarge AWS instance with a Graviton3 processor clocked at 2.6GHz and 512GB of RAM. We integrate Orion into the PyTorch framework; Orion generates the required FHE code and configuration parameters to run these networks under FHE. This representation could then be interpreted by many of the standard FHE libraries, and here we target Lattigo v4.1 as our backend. To make a fair comparison with prior work, we rerun Lee et al. [29] and Kim et al. [30] on the same instance. Reported latencies are singled-threaded and averaged over 20 distinct trials.

B. Microbenchmarks

Despite the growing interest in FHE applications, we find that there is still a lack of support for a concrete set of microbenchmarks that explore the tradeoff between level consumption and slot utilization. FHE parameter choice and tensor shape can have a large impact on performance. Therefore, we begin our evaluation with microbenchmarks to build intuition about the strengths of Orion, and will release these implementations (along with the neural networks presented next) to facilitate commensurable FHE neural inference research moving forward.

We develop a class of microbenchmarks that fall into three distinct categories: **Traditional** kernels reflect common operations found in standard CNNs. These include same-style (i.e., padded) convolutions on power-of-two input sizes, strided convolutions, and wide fully-connected layers. **Challenge** kernels stress compiler flexibility and performance with non-power-of-two input sizes, non-square kernels, and arbitrary padding. We find these kernels to be the most difficult to support as they introduce non-uniform slot utilization in the resulting ciphertexts. **Batched** operations pack multiple inputs into one ciphertext. As multi-key homomorphic schemes [31],

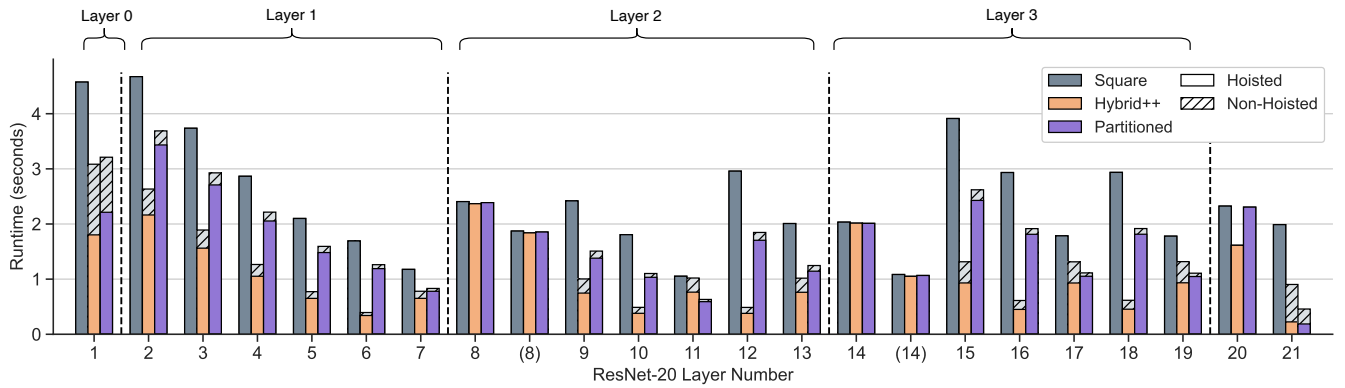


Fig. 7: Breakdown of ResNet-20 layer runtimes for the three proposed mapping strategies.

[32] become more prevalent, we expect the importance of batched inferences to grow as well.

As discussed in Section III, levels can highly impact runtime. Therefore, we run each kernel at three different levels, $L = L_{\min}$, 8, and 16 to rigorously compare our mapping strategies. Here, L_{\min} is the minimum level that the kernel can be computed for the respective mapping strategies. Recall that our Hybrid++ method necessarily consumes two levels per convolution due to the auxiliary repair matrix required to realign and mask data for the following layer. In contrast, our Partitioned method only requires one level at the expense of lower slot utilization. Therefore, L_{\min} is 1 for Partitioned (and Square) and 2 for Hybrid++ approach. In all cases, we set $N = 2^{16}$, which is a standard polynomial ring degree for FHE applications that require bootstrapping [29], [30].

Figure 6 details our nine microbenchmarks and reports their runtimes on the three mapping strategies proposed in Section III. We make key observations through our microbenchmarks that determine our choice of optimal mapping strategies in our neural network evaluation.

First, despite a lower slot utilization, our Partitioned method consistently outperforms the Hybrid++ (and Square) method at L_{\min} . This outcome is counter-intuitive given that prior work optimizes for slot utilization (e.g., Gazelle [26] and Lee et al. [29]). However, the necessary repair matrix in the Hybrid++ method introduces a trade-off between level consumption and slot utilization. Although the Hybrid++ method is more tightly packed, it consumes twice the level as Partitioned, thus doubling the amount of computation required for the same calculation. **Therefore, packing data as tightly as possible in order to minimize the total number of rotations is not equivalent to minimizing runtime in FHE settings.**

Second, strided convolutions are expensive (often $4\times$ slower than their non-strided counterparts). Recall from Section III that regardless of mapping strategy, $L_{\min} = 2$, since we must undo the multiplexed packing technique for future layers. Heuristically, we find that the Square method minimizes the aggregate runtime of strided convolutions in part due to a substantially simpler repair matrix, and therefore adopt the Square approach for all strided convolutions going forward. Furthermore, Orion attempts to perform strided convolutions

at the lowest level possible. This entails judiciously mapping the locations of Bootstrap operations.

C. Benchmarks

We evaluate Orion on a range of convolutional and fully-connected neural networks. Our network architectures are as follows. **MLP** is a three-layer fully-connected network from SecureML [33] for MNIST [34]. This network is used in prior work [26], [35] and represents a starting point for our evaluation. **LoLA** is a three-layer convolutional neural network from LoLA-CryptoNets [36] also targeting MNIST. LoLA is our simplest CNN architecture that consists of one strided convolution and two fully-connected layers. **LeNet (Large)** [34] is a four-layer convolutional neural network adopted from CHET [9] and EVA [10]. It is the largest of their LeNet benchmarks and consists of two strided-convolutions followed by two fully-connected layers. We modify LeNet for CIFAR10 rather than MNIST to make it more challenging. **ResNets** [37] have seen widespread success in computer vision tasks. ResNets are also the most complicated neural networks supported by prior hand-crafted FHE solutions. We evaluate the ResNet-20 architecture on CIFAR10 and ResNet-32 on CIFAR100, similar to [29].

Table II reports the runtime of each neural network for all three mapping strategies alongside relevant CKKS parameters. We detail several high-level insights and observations before exploring the ResNet results in more detail. First, even our smallest benchmark, MLP, requires a polynomial ring degree, $N = 2^{14}$ to remain 128-bit secure. This is vastly more slots than required, therefore small networks such as these are ideal for batching. Second, we note the differences in maximum multiplicative level, L , between mapping strategies. In networks that do not require bootstrapping, our Hybrid++ approach requires *more* levels than than Square and Partitioned. This is the result of the repair matrix. Moreover, the increase in multiplicative depth leads the Hybrid++ method to consistently perform worse than Partitioned, and sometimes even worse than Square. Finally, we observe latencies that are $15\times$ and $30\times$ lower than the single-threaded results reported in EVA and CHET, respectively. While there have been several advancements to FHE algorithms since its publication [12],

[13], we suspect a large fraction of speedup stems from Orion’s support for hoisted rotations.

We now analyze the results of our ResNet-20 implementation in detail and compare against prior hand-crafted solutions. We divide each linear and convolutional layer into two segments: one section in which hoisted rotations are employed to compute the necessary matrix-vector products and another for operations where hoisting is not possible (e.g., input duplication and output rotations). Figure 7 shows the per-layer ResNet-20 runtime for all three methods and is divided into the hoisted and non-hoisted segments.

We note that Square avoids performing any non-hoisted operations, albeit at the cost of consistency higher runtimes compared to the Hybrid++ and Partitioned methods. This is because Square over-provisions unnecessary hoisted rotations and often exhibits poor slot utilization that leads to high layer runtimes. On the other hand, Hybrid++ and Partitioned optimize for both slot utilization and hoisted rotations.

Additionally, we see that the Hybrid++ method exhibits the lowest per-layer latency. However, this method is bottlenecked by an increase in Bootstrap operations due to the auxiliary repair matrix consuming an additional level. While this may initially seem at odds with our microbenchmark results, we find that an increased frequency in bootstrapping results in Hybrid++ convolutions being performed at lower levels than the Square and Partitioned alternatives accounting for the performance differences.

Table III further breaks down ResNet-20 inference latency into the time for convolutional layers, activation functions, Bootstrap operations, and linear layers. We rerun the work by Lee et al. [29] and Kim et al. [30] for a fair comparison and report their runtimes on the same operations. We also port the network architecture and CKKS parameters from Lee et al. [29], denoted as Lee (Opt.) in Table III, to Lattigo to better understand the balance between convolutional and Bootstrap runtimes. We find that Orion outperforms both state-of-the-art rotation-based and FFT-based solutions.

First, although FFT-based solutions are mostly rotation-free (i.e., avoid expensive key-switching operations), they necessitate bootstrapping after every convolution, regardless of the activation function. Therefore, the bootstrapping runtime observed from Kim et al. [30] in Table III establishes a hard lower-bound on their latency. Orion avoids this by taking a rotation-based approach, similar to Lee et al. [29]. This gives us the flexibility to choose the levels at which convolutions are performed and the locations of Bootstrap operations to further decrease latency. This performance increase can be observed in Table III, where all three of Orion’s mapping strategies achieve 2–3× lower latencies than just the Bootstrap runtimes of Kim et al. [30], despite an increase in convolutional runtime.

Second, although the convolutional runtime of Hybrid++ is faster than Partitioned, the increase in Bootstrap operations from 5 to 8 results in an overall higher latency. This further emphasizes that minimizing level consumption is as important as maximizing slot utilization in FHE.

Finally, we compare the performance of Orion to the prior

TABLE II: Network architectures and runtimes.

| Network | Method | N | L | $\log QP$ | Bootstraps | Runtime (s) |
|-------------------|--------|----------|-----|-----------|------------|-------------|
| MLP [33] | S | 2^{14} | 7 | 437 | 0 | 1.09 |
| | H++ | | 9 | 419 | | 1.21 |
| | P | | 7 | 437 | | 0.62 |
| LoLA [36] | S | 2^{14} | 8 | 428 | 0 | 1.91 |
| | H++ | | 9 | 419 | | 1.48 |
| | P | | 8 | 428 | | 1.29 |
| LeNet (Large) [9] | S | 2^{15} | 11 | 847 | 0 | 14.4 |
| | H++ | | 12 | 831 | | 9.33 |
| | P | | 11 | 847 | | 9.12 |
| ResNet-20 [37] | S | 2^{16} | 26 | 1521 | 5 | 155.6 |
| | H++ | | 26 | 1521 | 8 | 181.4 |
| | P | | 26 | 1521 | 5 | 139.7 |
| ResNet-32 [37] | S | 2^{16} | 26 | 1521 | 9 | 287.9 |
| | H++ | | 26 | 1521 | 14 | 312.1 |
| | P | | 26 | 1521 | 9 | 260.1 |

state-of-the-art rotation-based approach of Lee et al. [29]. Similar to Kim et al. [30], Lee et al. [29] perform convolutions at the lowest level possible (i.e., L_{\min}). This is primarily due to their use of high-degree polynomials to approximate the ReLU activation function. Despite Orion performing convolutions at much higher levels, we still see roughly a 15× and 11× improvement in convolutional runtimes in the Hybrid++ and Partitioned methods, respectively. In total, we observe over a 20× speedup in end-to-end latency compared to Lee et al. [29]. We supplement our analysis by replicating the network architecture and CKKS parameters from Lee et al. to perform convolutions at L_{\min} . Here, we apply the Hybrid++ approach to all convolutions, and focus on the trade-off between convolutional and bootstrapping runtimes. From this, we gain two key insights: 1) bootstrapping once again dominates runtime, similar to Kim et al. [30]. Therefore rotation-based approaches are ideal when coupled with the use of lower degree polynomials as activation functions, which afford a greater flexibility in the choice of Bootstrap locations, and 2) Lee et al. [29] optimize for convolutional runtime at the expense of end-to-end latency. This is seen in Table III by comparing the Bootstrap runtime of our optimized implementation of Lee et al. with all three of Orion’s proposed mapping strategies. This latency difference suggests that to better balance the trade-off between convolutional and Bootstrap runtime (i.e., minimize end-to-end latency), convolutions must necessarily be performed at higher levels than all prior work.

D. Dense Packing and Non-Hoisted Rotations

We close with an observation about our Hybrid++ method. Recall from Section III that when possible, this method packs multiple copies of the same input into one ciphertext, thereby increasing slot utilization. In this case, however, increasing slot utilization comes at the cost of increasing the amount of non-hoisted rotations both in terms of input packing and output rotations. Therefore, a natural question to ask is whether we *should* be tightly packing data, or if the increase in expensive non-hoisted rotations negates any potential improvements.

TABLE III: ResNet-20 comparison with prior work.

| ResNet-20 Breakdown (secs.) | FFT-Based | Rotation-Based | | | | |
|-----------------------------|------------------|------------------|--------------|--------------|--------------|--------------|
| | Kim et. al. [30] | Lee et. al. [29] | Lee (Opt.) | Orion (S) | Orion (H++) | Orion (P) |
| Conv. | 9.88 | 438.6 | 18.25 | 54.2 | 28.9 | 40.4 |
| Act. | 53.78 | 244.5 | 3.34 | 3.45 | 3.14 | 3.45 |
| Boot. | 282.5 | 2138 | 344.6 | 92.6 | 144.6 | 92.0 |
| Linear | 3.52 | 14.52 | 0.89 | 1.99 | 0.90 | 0.46 |
| Other | 21.69 | 29.11 | 0.21 | 3.41 | 3.85 | 3.40 |
| Total (s) | 371.4 | 2864 | 367.3 | 155.6 | 181.4 | 139.7 |

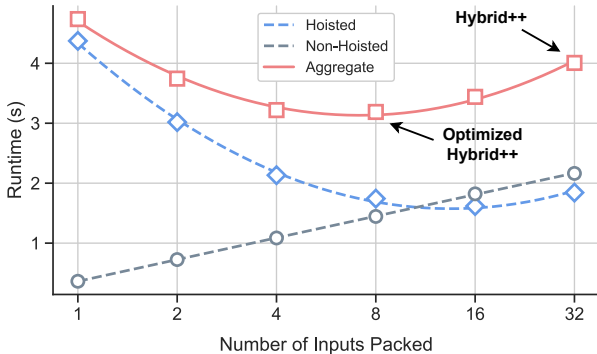


Fig. 8: Packing density versus latency for Hybrid++.

We illustrate this trade-off with the 256×1024 FC microbenchmark with $L = 16$ and $N = 2^{16}$ ($n = 2^{15}$). Recall from Section III that when $n_o < n$, we can pack n/n_o many copies of the same input into one ciphertext to utilize all available slots; here, $n/n_o = 32$. We explore the impact of more sparsely packing slots by varying this value from 1 up to 32 in Figure 8. We plot both hoisted and non-hoisted latencies as well as their aggregate runtime. Notably, past a certain point, the reduction in latency from a more tightly packed ciphertext is offset by an *increase* in latency from performing more non-hoisted rotations. The Hybrid++ method, as described in Section III, greedily packs the ciphertext and moves beyond the optimal strategy as shown in Figure 8. For this microbenchmark, we find that the optimal number of inputs to pack in order to minimize runtime latency is 8 copies of the input (Optimized Hybrid++), which results in 75% of slots going unused. This optimization, albeit counter-intuitive, is natively supported by Orion.

V. RELATED WORK

Prior work broadly falls into three categories: FHE-only, hybrid, and compiler-based solutions. Table IV summarizes key prior literature.

For FHE-based protocols, Cryptonets [38] was the seminal paper introducing private neural network inference via FHE and adopted the use of FHE-amenable polynomial activation functions. Following this work, several optimizations to data layouts were proposed to both reduce latency and increase throughput [36], [39]. Since then, Lee et al. [28], [29] proposed high-degree polynomial activation functions in order

TABLE IV: Comparison of Prior Work.

| Prior Work | Auto-mated | FHE Only | Deep Networks | Batching Support | Arbitrary Convolutions |
|---------------------|------------|----------|---------------|------------------|------------------------|
| Lee et al. [29] | ○ | ● | ● | ○ | ● |
| Kim et al. [30] | ○ | ● | ● | ● | ● |
| HYPHEN [25] | ○ | ● | ● | ○ | ○ |
| Gazelle [26] | ● | ○ | ● | ● | ● |
| Cheetah [40] | ● | ○ | ● | ● | ● |
| SlytHERin [28] | ● | ○ | ● | ● | ● |
| CHET [9] | ● | ● | ○ | ○ | ○ |
| EVA [10] | ● | ● | ○ | ○ | ○ |
| HeLayers [44] | ● | ● | ○ | ○ | ○ |
| HEMET [45] | ● | ● | ○ | ○ | ○ |
| Porcupine [7] | ● | ● | ○ | ○ | ○ |
| Coyote [8] | ● | ● | ○ | ○ | ○ |
| HECO [11] | ● | ● | ○ | ○ | ○ |
| Orion (ours) | ● | ● | ● | ● | ● |

to support deeper networks such as ResNets. HYPHEN [25] uses low-degree polynomials and reduces the number of HE rotations for their linear algebra kernels. Finally, Kim et al. [30] avoids rotations entirely by using an FFT-based solution at the cost of introducing a large number of bootstrap operations.

Besides FHE-only solutions, SecureML [33] proposed a hybrid protocol for private inference, which leveraged FHE for the linear layers and multi-party computations (MPC) protocols for non-linear functions prevalent in standard CNNs such as ReLU. Gazelle [26] further expanded upon the work of SecureML [33] by proposing several packing strategies for rotation-based matrix-vector products for computing convolutions and fully-connected layers. Cheetah [40] proposed both SIMD-Free and Rotation-Free FHE algorithms, but still employ communication-heavy MPC protocols for computing ReLU. Several prior works also focus on compiler design in order to lower the barrier of entry for deploying FHE. CHET [9] builds a domain-specific language to automatically generate a set of FHE primitives for a given neural network and systematically explores the FHE parameter space to outperform manually written FHE programs. EVA [10] extends the work of CHET by optimizing FHE level consumption to further reduce HE runtime. CHET and EVA specifically target neural network inference, and compilers that target arbitrary FHE programs also exist [7], [8], [11]. Most compilers build on top of existing FHE frameworks, e.g., Lattigo [15], SEAL [41], HELib [42], OpenFHE [43], HEAAN [16].

VI. CONCLUSION

Recent advancements in Fully Homomorphic Encryption continue to push the field into the realm of practicality. And while prior work has shown promising solutions to the use of FHE for neural network inference, they have been unable able to fully realize the potential of existing FHE techniques due to complexities such as limited programmability, parameter selection, and slot utilization, which often require expert knowledge. Our solution, Orion, solves each

of these issues by allowing practitioners to work in an accessible language such as PyTorch and automatically balances many of the aforementioned FHE intricacies. Furthermore, our compiler-based approach outperforms hand-crafted solutions while remaining general purpose and supports arbitrarily deep networks. Furthermore through our analysis, we find counter-intuitive tradeoffs between slot utilization, level consumption, and bootstrapping management. In particular, packing data as tightly as possible in order to minimize the total number of rotations is not equivalent to minimizing runtime in FHE settings. Finally, we hope that by open-sourcing Orion, we ease the development of FHE-based neural network systems for practitioners and better inform the community about the unique challenges and opportunities present in FHE.

ACKNOWLEDGEMENTS

This work was supported in part by Graduate Assistance in Areas of National Need (GAANN). The research was developed with funding from DARPA, under the Data Protection in Virtual Environments (DPRIVE) program, contract HR0011-21-9-0003. Reagen and Ebel received generous support from the NY State Center for Advanced Technology in Telecommunications (CATT) and a gift award from Google. We especially thank Jean-Phillipe Bossuat for the insightful discussions and valuable feedback. The views, opinions, and/or findings expressed are those of the authors and do not necessarily reflect the views of sponsors.

REFERENCES

- [1] B. Reagen, W.-S. Choi, Y. Ko, V. T. Lee, H.-H. S. Lee, G.-Y. Wei, and D. Brooks, “Cheetah: Optimizing and accelerating homomorphic encryption for private inference,” in *2021 IEEE International Symposium on High-Performance Computer Architecture (HPCA)*, 2021, pp. 26–39.
- [2] A. Feldmann, N. Samardzic, A. Krastev, S. Devadas, R. Dreslinski, K. Eldefrawy, N. Genise, C. Peikert, and D. Sanchez, “F1: A fast and programmable accelerator for fully homomorphic encryption (extended version),” 2021.
- [3] S. Kim, J. Kim, M. J. Kim, W. Jung, J. Kim, M. Rhu, and J. H. Ahn, “BTS,” in *Proceedings of the 49th Annual International Symposium on Computer Architecture*. ACM, jun 2022. [Online]. Available: <https://doi.org/10.1145%2F3470496.3527415>
- [4] N. Samardzic, A. Feldmann, A. Krastev, N. Manohar, N. Genise, S. Devadas, K. Eldefrawy, C. Peikert, and D. Sanchez, “Craterlake: A hardware accelerator for efficient unbounded computation on encrypted data,” in *Proceedings of the 49th Annual International Symposium on Computer Architecture*, ser. ISCA ’22. New York, NY, USA: Association for Computing Machinery, 2022, p. 173–187. [Online]. Available: <https://doi.org/10.1145/3470496.3527393>
- [5] D. Soni, N. Neda, N. Zhang, B. Reynwar, H. Gamil, B. Heyman, M. Nabeel, A. A. Badawi, Y. Polyakov, K. Canida, M. Pedram, M. Maniatakos, D. B. Cousins, F. Franchetti, M. French, A. Schmidt, and B. Reagen, “Rpu: The ring processing unit,” 2023.
- [6] J. Kim, S. Kim, J. Choi, J. Park, D. Kim, and J. H. Ahn, “Sharp: A short-word hierarchical accelerator for robust and practical fully homomorphic encryption,” in *Proceedings of the 50th Annual International Symposium on Computer Architecture*, ser. ISCA ’23. New York, NY, USA: Association for Computing Machinery, 2023. [Online]. Available: <https://doi.org/10.1145/3579371.3589053>
- [7] M. Cowan, D. Dangwal, A. Alaghi, C. Trippel, V. T. Lee, and B. Reagen, “Porcupine: A synthesizing compiler for vectorized homomorphic encryption,” in *Proceedings of the 42nd ACM SIGPLAN International Conference on Programming Language Design and Implementation*, ser. PLDI 2021. New York, NY, USA: Association for Computing Machinery, 2021, p. 375–389. [Online]. Available: <https://doi.org/10.1145/3453483.3454050>
- [8] R. Malik, K. Sheth, and M. Kulkarni, “Coyote: A compiler for vectorizing encrypted arithmetic circuits,” in *Proceedings of the 28th ACM International Conference on Architectural Support for Programming Languages and Operating Systems, Volume 3*, ser. ASPLOS 2023. New York, NY, USA: Association for Computing Machinery, 2023, p. 118–133. [Online]. Available: <https://doi.org/10.1145/3582016.3582057>
- [9] R. Dathathri, O. Saarikivi, H. Chen, K. Laine, K. Lauter, S. Maleki, M. Musuvathi, and T. Mytkowicz, “Chet: An optimizing compiler for fully-homomorphic neural-network inferencing,” in *Proceedings of the 40th ACM SIGPLAN Conference on Programming Language Design and Implementation*, ser. PLDI 2019. New York, NY, USA: Association for Computing Machinery, 2019, p. 142–156. [Online]. Available: <https://doi.org/10.1145/3314221.3314628>
- [10] R. Dathathri, B. Kostova, O. Saarikivi, W. Dai, K. Laine, and M. Musuvathi, “EVA: an encrypted vector arithmetic language and compiler for efficient homomorphic computation,” in *Proceedings of the 41st ACM SIGPLAN Conference on Programming Language Design and Implementation*. ACM, jun 2020. [Online]. Available: <https://doi.org/10.1145%2F3385412.3386023>
- [11] A. Viand, P. Jattke, M. Haller, and A. Hithnawi, “Heco: Fully homomorphic encryption compiler,” 2023.
- [12] K. Han and D. Ki, “Better bootstrapping for approximate homomorphic encryption,” in *Topics in Cryptology – CT-RSA 2020: The Cryptographers’ Track at the RSA Conference 2020, San Francisco, CA, USA, February 24–28, 2020, Proceedings*. Berlin, Heidelberg: Springer-Verlag, 2020, p. 364–390. [Online]. Available: https://doi.org/10.1007/978-3-030-40186-3_16
- [13] J.-P. Bossuat, C. Mouchet, J. Troncoso-Pastoriza, and J.-P. Hubaux, “Efficient bootstrapping for approximate homomorphic encryption with non-sparse keys,” in *Advances in Cryptology – EUROCRYPT 2021*, A. Canteaut and F.-X. Standaert, Eds. Cham: Springer International Publishing, 2021, pp. 587–617.
- [14] A. Paszke, S. Gross, F. Massa, A. Lerer, J. Bradbury, G. Chanan, T. Killeen, Z. Lin, N. Gimelshein, L. Antiga, A. Desmaison, A. Köpf, E. Yang, Z. DeVito, M. Raison, A. Tejani, S. Chilamkurthy, B. Steiner, L. Fang, J. Bai, and S. Chintala, “Pytorch: An imperative style, high-performance deep learning library,” 2019.
- [15] “Lattigo v4,” Online: <https://github.com/tuneinsight/lattigo>, Aug. 2022, ePFL-LDS, Tune Insight SA.
- [16] J. H. Cheon, A. Kim, M. Kim, and Y. Song, “Homomorphic encryption for arithmetic of approximate numbers,” in *Advances in Cryptology–ASIACRYPT 2017: 23rd International Conference on the Theory and Applications of Cryptology and Information Security, Hong Kong, China, December 3-7, 2017, Proceedings, Part I 23*. Springer, 2017, pp. 409–437.
- [17] C. Gentry, “Fully homomorphic encryption using ideal lattices,” in *Proceedings of the forty-first annual ACM symposium on Theory of computing*, 2009, pp. 169–178.
- [18] Z. Brakerski, C. Gentry, and V. Vaikuntanathan, “(leveled) fully homomorphic encryption without bootstrapping,” in *Proceedings of the 3rd Innovations in Theoretical Computer Science Conference*, ser. ITCS ’12. New York, NY, USA: Association for Computing Machinery, 2012, p. 309–325. [Online]. Available: <https://doi.org/10.1145/2090236.2090262>
- [19] Z. Brakerski, “Fully homomorphic encryption without modulus switching from classical gapsvp,” in *Advances in Cryptology – CRYPTO 2012*, R. Safavi-Naini and R. Canetti, Eds. Berlin, Heidelberg: Springer Berlin Heidelberg, 2012, pp. 868–886.
- [20] J. Fan and F. Vercauteren, “Somewhat practical fully homomorphic encryption,” *Cryptology ePrint Archive*, Paper 2012/144, 2012, <https://eprint.iacr.org/2012/144>. [Online]. Available: <https://eprint.iacr.org/2012/144>
- [21] V. Lyubashevsky, C. Peikert, and O. Regev, “On ideal lattices and learning with errors over rings,” in *Advances in Cryptology–EUROCRYPT 2010: 29th Annual International Conference on the Theory and Applications of Cryptographic Techniques, French Riviera, May 30–June 3, 2010. Proceedings 29*. Springer, 2010, pp. 1–23.
- [22] S. Halevi and V. Shoup, “Algorithms in helib,” *Cryptology ePrint Archive*, Paper 2014/106, 2014, <https://eprint.iacr.org/2014/106>. [Online]. Available: <https://eprint.iacr.org/2014/106>
- [23] K. Garimella, N. K. Jha, and B. Reagen, “Sisyphus: A cautionary tale of using low-degree polynomial activations in privacy-preserving

- deep learning,” in *ACM CCS Workshop on Private-preserving Machine Learning*, 2021.
- [24] J. Park, M. J. Kim, W. Jung, and J. H. Ahn, “Aespa: Accuracy preserving low-degree polynomial activation for fast private inference,” 2022.
- [25] D. Kim, J. Park, J. Kim, S. Kim, and J. H. Ahn, “Hyphen: A hybrid packing method and optimizations for homomorphic encryption-based neural networks,” 2023.
- [26] C. Juvekar, V. Vaikuntanathan, and A. Chandrakasan, “GAZELLE: A low latency framework for secure neural network inference,” in *27th USENIX Security Symposium (USENIX Security 18)*. Baltimore, MD: USENIX Association, Aug. 2018, pp. 1651–1669. [Online]. Available: <https://www.usenix.org/conference/usenixsecurity18/presentation/juvekar>
- [27] M. Gnacik and K. Łapa, “Using toeplitz matrices to obtain 2d convolution,” 10 2022.
- [28] F. Intoci, S. Sav, A. Pyrgelis, J.-P. Bossuat, J. R. Troncoso-Pastoriza, and J.-P. Hubaux, “slytherin: An agile framework for encrypted deep neural network inference,” 2023.
- [29] E. Lee, J.-W. Lee, J. Lee, Y.-S. Kim, Y. Kim, J.-S. No, and W. Choi, “Low-complexity deep convolutional neural networks on fully homomorphic encryption using multiplexed parallel convolutions,” in *Proceedings of the 39th International Conference on Machine Learning*, ser. Proceedings of Machine Learning Research, K. Chaudhuri, S. Jegelka, L. Song, C. Szepesvari, G. Niu, and S. Sabato, Eds., vol. 162. PMLR, 17–23 Jul 2022, pp. 12 403–12 422. [Online]. Available: <https://proceedings.mlr.press/v162/lee22e.html>
- [30] D. Kim and C. Guyot, “Optimized privacy-preserving cnn inference with fully homomorphic encryption,” *IEEE Transactions on Information Forensics and Security*, vol. 18, pp. 2175–2187, 2023.
- [31] H. Chen, W. Dai, M. Kim, and Y. Song, “Efficient multi-key homomorphic encryption with packed ciphertexts with application to oblivious neural network inference,” in *Proceedings of the 2019 ACM SIGSAC Conference on Computer and Communications Security*, 2019, pp. 395–412.
- [32] J. Ma, S.-A. Naas, S. Sigg, and X. Lyu, “Privacy-preserving federated learning based on multi-key homomorphic encryption,” *International Journal of Intelligent Systems*, vol. 37, no. 9, pp. 5880–5901, 2022.
- [33] P. Mohassel and Y. Zhang, “Secureml: A system for scalable privacy-preserving machine learning,” *Cryptology ePrint Archive*, Paper 2017/396, 2017, <https://eprint.iacr.org/2017/396>. [Online]. Available: <https://eprint.iacr.org/2017/396>
- [34] Y. Lecun, L. Bottou, Y. Bengio, and P. Haffner, “Gradient-based learning applied to document recognition,” *Proceedings of the IEEE*, vol. 86, no. 11, pp. 2278–2324, 1998.
- [35] J. Liu, M. Juuti, Y. Lu, and N. Asokan, “Oblivious neural network predictions via minionn transformations,” in *Proceedings of the 2017 ACM SIGSAC Conference on Computer and Communications Security*, ser. CCS ’17. New York, NY, USA: Association for Computing Machinery, 2017, p. 619–631. [Online]. Available: <https://doi.org/10.1145/3133956.3134056>
- [36] A. Brutzkus, O. Elisha, and R. Gilad-Bachrach, “Low latency privacy preserving inference,” in *International Conference on Machine Learning*, 2019.
- [37] K. He, X. Zhang, S. Ren, and J. Sun, “Deep residual learning for image recognition,” 2015.
- [38] R. Gilad-Bachrach, N. Dowlin, K. Laine, K. Lauter, M. Naehrig, and J. Wernsing, “Cryptonets: Applying neural networks to encrypted data with high throughput and accuracy,” in *Proceedings of The 33rd International Conference on Machine Learning*, ser. Proceedings of Machine Learning Research, M. F. Balcan and K. Q. Weinberger, Eds., vol. 48. New York, New York, USA: PMLR, 20–22 Jun 2016, pp. 201–210. [Online]. Available: <https://proceedings.mlr.press/v48/gilad-bachrach16.html>
- [39] E. Chou, J. Beal, D. Levy, S. Yeung, A. Haque, and L. Fei-Fei, “Faster cryptonets: Leveraging sparsity for real-world encrypted inference,” 2018.
- [40] Z. Huang, W. jie Lu, C. Hong, and J. Ding, “Cheetah: Lean and fast secure two-party deep neural network inference,” *Cryptology ePrint Archive*, Paper 2022/207, 2022, <https://eprint.iacr.org/2022/207>. [Online]. Available: <https://eprint.iacr.org/2022/207>
- [41] “Microsoft SEAL (release 4.1),” <https://github.com/Microsoft/SEAL>, Jan. 2023, microsoft Research, Redmond, WA.
- [42] S. Halevi and V. Shoup, “Design and implementation of helib: a homomorphic encryption library,” *Cryptology ePrint Archive*, Paper 2020/1481, 2020, <https://eprint.iacr.org/2020/1481>. [Online]. Available: <https://eprint.iacr.org/2020/1481>
- [43] A. A. Badawi, J. Bates, F. Bergamaschi, D. B. Cousins, S. Erabelli, N. Genise, S. Halevi, H. Hunt, A. Kim, Y. Lee, Z. Liu, D. Micciancio, I. Quah, Y. Polyakov, S. R.V., K. Rohloff, J. Saylor, D. Suponitsky, M. Triplett, V. Vaikuntanathan, and V. Zucca, “Openfhe: Open-source fully homomorphic encryption library,” *Cryptology ePrint Archive*, Paper 2022/915, 2022, <https://eprint.iacr.org/2022/915>. [Online]. Available: <https://eprint.iacr.org/2022/915>
- [44] E. Aharoni, A. Adir, M. Baruch, N. Drucker, G. Ezov, A. Farkash, L. Greenberg, R. Masalha, G. Moshkovich, D. Murik, H. Shaul, and O. Soceanu, “HeLayers: A tile tensors framework for large neural networks on encrypted data,” *Proceedings on Privacy Enhancing Technologies*, vol. 2023, no. 1, pp. 325–342, jan 2023. [Online]. Available: <https://doi.org/10.56553/2Fpoptes-2023-0020>
- [45] Q. Lou and L. Jiang, “Hemet: A homomorphic-encryption-friendly privacy-preserving mobile neural network architecture,” 2021.